Transport properties of the topological Kondo insulator SmB_6 under the irradiation of light*

Guo-Bao Zhu(朱国宝)[1,2] and Hui-Min Yang(杨慧敏)[1,†]

[1] *Department of Physics and Electronic Engineering, Heze University, Heze* 274015, *China*
[2] *Institute of Theoretical Physics, Heze University, Heze* 274015, *China*

(Received 25 April 2016; revised manuscript received 6 June 2016; published online 25 August 2016)

In this paper, we study transport properties of the $\overline{X}$ point in the Brillouin zone of the topological Kondo insulator SmB_6 under the application of a circularly polarized light. The transport properties at high-frequency regime and low-frequency regime as a function of the ratio (κ) of the Dresselhaus-like and Rashba-like spin–orbit parameter are studied based on the Floquet theory and Boltzmann equation respectively. The sign of Hall conductivity at high-frequency regime can be reversed by the ratio κ and the amplitude of the light. The amplitude of the current can be enhanced by the ratio κ. Our findings provide a way to control the transport properties of the Dirac materials at low-frequency regime.

Keywords: SmB_6, light, Flouqet theory, Boltzmann equation

PACS: 73.43.–f, 78.67.–n **DOI:** 10.1088/1674-1056/25/10/107303

1. Introduction

In the past few years, topological insulators[1,2] have attracted significant interest in condensed matter physics both in theory and experiment. A weakly interacting system with strong spin–orbit coupling and insulators driven by strong electron correlations can result in a topological insulating state. The narrow gap insulator in which the gap is created by electron correlations are called topological Kondo insulators. The first well-known topological Kondo insulator material is SmB_6.[3–5] The topological properties of SmB_6 have been studied extensively both theoretically and experimentally.[5–13] Lu *et al.*[5] have found non-trivial Z_2 topology in typical mixed valence SmB_6 based on first-principles calculations. Kim *et al.*[11] have investigated the surface in-gap states in a potential mixed-valent SmB_6 based on first-principles density functional theory. In Refs. [12] and [13], the authors studied the properties of topologically protected surface states in SmB_6, and found that there are four different topological phases in SmB_6, which are distinguished by the sign of mirror Chern numbers. Transport properties of surface stats in the material that are poorly understood.

Different experiments have shown that transport is indeed dominated by the surface contributions at low temperature.[14–16] In Ref. [17], the authors provided conclusive evidence for surface-dominated transport in SmB_6 at low temperature. The spin- and angle-resolved photoemission spectroscopy measurements showed that the surface states of SmB_6 around the $\overline{X}$ point are spin-polarized.[18] The surface states of SmB_6 around the $\overline{X}$ point can be described by a combination of Rashba- and Dresselhaus-like spin–orbit Hamiltonian.[19,20] The interplay between the Rashba and Dresselhaus parameters on transport properties is studied in our paper.

Generally speaking, the effect of light irradiation on electron systems are photon-dressing of band structures through the mixing of different bands and redistribution of electron occupation numbers through the absorptions/emissions of photons leading to non equilibrium distributions.[21] In this paper, we use the Floquet theory and linearized Boltzmann equation to analyze the influence of light on transport properties of SmB_6 in low-frequency and high-frequency limit, respectively.

The structure of this paper is organized as follows. In Section 2 we present a brief account of the effective Hamiltonian with a circularly polarized light. Based on the Floquet theory, we study the transport properties of our model at high frequency in Section 3. In Section 4, we study the transport properties of our model at low frequency by solving the Boltzmann equation. In Section 5, we summarize our results.

2. Model Hamiltonian

Based on $k \cdot p$ theory and density functional theory, the low energy physics of the surface states of an ultrathin slab of SmB_6 at the $\overline{X}$ point can be captured by the following Hamiltonian[19,20]

$$H_0 = \alpha_R \boldsymbol{\sigma} \times \boldsymbol{k} \cdot I_z + \alpha_D \boldsymbol{\sigma} \cdot \boldsymbol{k} + \Delta \sigma_z, \tag{1}$$

where $\alpha_{R,D}$ are the Rashba- and Dresselhaus-like coupling coefficients respectively. $\boldsymbol{\sigma} = (\hat{\sigma}_x, \hat{\sigma}_y, \hat{\sigma}_z)$ are Pauli matrices.

*Project supported by the National Natural Science Foundation of China (Grant Nos. 11504095 and 11447145), the Foundation of Heze University (Grant Nos. XY14B002 and XYPY01), and the Project funded by the Higher Educational Science and Technology Program of Shandong Province, China (Grant No. J15LJ55).

†Corresponding author. E-mail: yangyhm2016@163.com

© 2016 Chinese Physical Society and IOP Publishing Ltd

$\boldsymbol{k} = (k_x, k_y, 0)$ are the momentum measured from the $\overline{X}$ point. I_z is 2×2 unit matrix vector in the z direction. Δ is the surface-hybridization induced band gap of the surface. The band dispersions relationship of the free Hamiltonian are

$$E_{\pm} = \pm\sqrt{\alpha^2 k^2 + \Delta^2}, \tag{2}$$

and the the corresponding wave functions are

$$u_{+\boldsymbol{k}} = \left[\cos\frac{\theta}{2}, \sin\frac{\theta}{2}\mathrm{e}^{-\mathrm{i}\varphi}\right]^{\mathrm{T}}, \tag{3}$$

$$u_{-\boldsymbol{k}} = \left[\sin\frac{\theta}{2}, -\cos\frac{\theta}{2}\mathrm{e}^{-\mathrm{i}\varphi}\right]^{\mathrm{T}}, \tag{4}$$

where

$$\alpha^2 = \alpha_{\mathrm{R}}^2 + \alpha_{\mathrm{D}}^2 + 2\alpha_{\mathrm{R}}\alpha_{\mathrm{D}}\sin(2\phi),$$
$$\tan\phi = k_y/k_x,$$
$$\cos\theta = \Delta/\sqrt{\alpha^2 k^2 + \Delta^2},$$

and $\tan\varphi = (k_x + \kappa k_y)/(k_y + \kappa k_x)$. $\kappa = \alpha_{\mathrm{D}}/\alpha_{\mathrm{R}}$ is the ratio between the Dresselhaus and Rashba coupling coefficients. When the Dresselhaus component is ignored ($\kappa = 0$), the model is reduced to massive Dirac model of the magnetically doped surface states of a three-dimensional (3D) topological insulator,[22] and the corresponding energy contours for E_+ are shown in Fig. 1(a). If the Rashba component is ignored, the model is reduced to the effective Hamiltonian for the electrons in graphene in the presence of sublattice potential.[23] When both α_{D} and α_{R} are nonzero, three different energy contours for E_+ are shown in Figs. 1(b)–1(d) as increasing of κ for small κ. The energy in Fig. 1 is plotted in units of α_{R}. The similar energy contours can be obtained when the unit of energy is α_{D}.

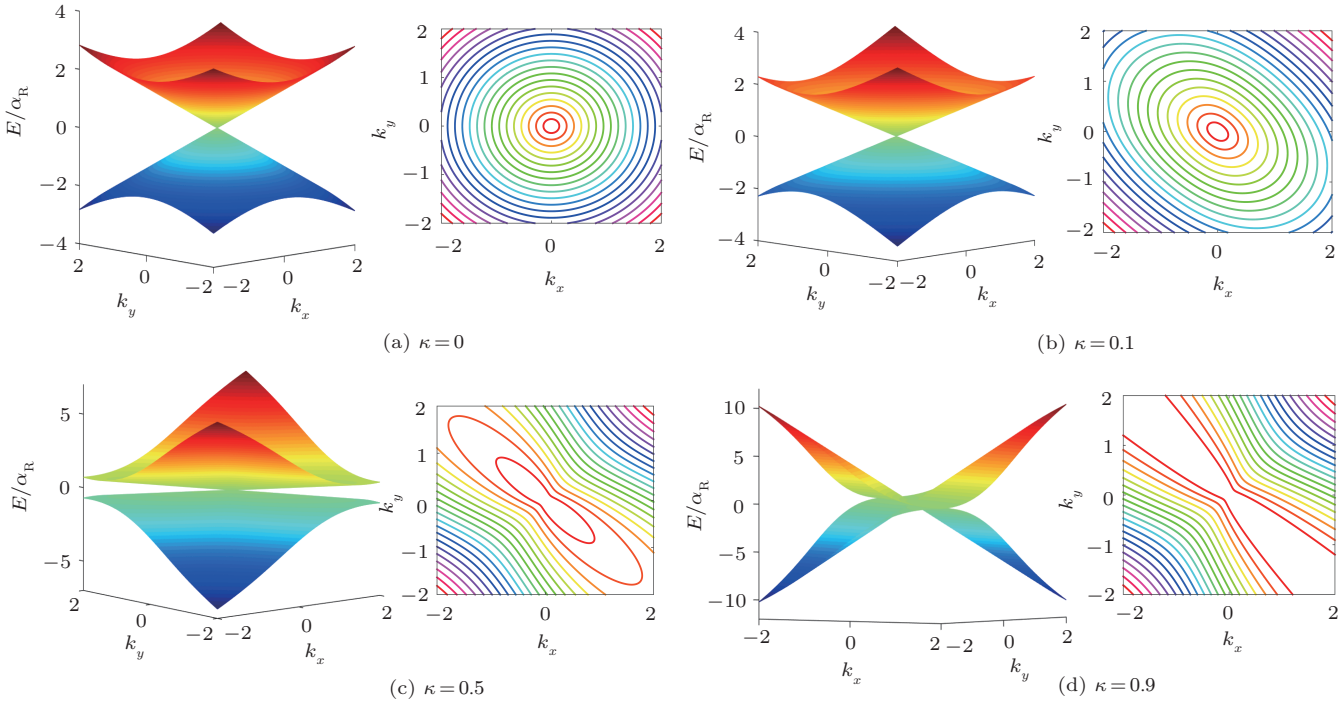


Fig. 1. (color online) Band structure at the X point and contour plot of the corresponding conduction band for fixed $\Delta = 0$ and different κ.

When the system under illumination by circularly polarized light represented by the time-dependent vector potential

$$\boldsymbol{A}(t) = A(\cos\omega t, \sin\omega t), \tag{5}$$

the time-dependent Hamiltonian is

$$H(t) = H_0 + \alpha_{\mathrm{R}}\boldsymbol{\sigma}\times\boldsymbol{A}(t)\cdot I_z + \alpha_{\mathrm{D}}\boldsymbol{\sigma}\cdot\boldsymbol{A}(t), \tag{6}$$

where $A = E_0/\omega$, E_0 and ω are the field strength and frequency respectively. The varied frequency and amplitude of the light can be used to control the dynamics of the system. In the high-frequency regime, the emission and absorption of a single virtual photon are enough to capture the energy dispersion and Floquet states based on the Floquet theory. Therefore, the dynamics of the system can be described by a time-independent effective Hamiltonian. In the low-frequency regime, there are more emissions and absorptions of photons to contribute to the transport. The photons lead the mixing of Floquet states and redistribution of electron occupation numbers. We use the Boltzmann transport equation to study the time evolution of the system. The two regimes are due to the two important physical effects of the application light. We focused on the analyses of the two effects in two regimes respectively.

3. Transport properties in the high-frequency regime

Previous works[24,25] proposed that light can dress the band structures of the system in the high frequency regime,

and the system can be described by static Hamiltonian. Based on the Floquet theory,[26–29] the static time-independent Hamiltonian is written as

$$H_{\rm eff} = H_0 + \frac{1}{\hbar\omega}[H_{-1}, H_1], \tag{7}$$

where

$$H_{\pm 1} = \frac{1}{T}\int_0^T {\rm d}t\, {\rm e}^{\pm {\rm i}\omega t} H(t), \tag{8}$$

in which $T = 2\pi/\omega$ is the time period of the light. The processes only include the emission and absorption of a single virtual photon. Then the effective Hamiltonian in the presence of light can be written as

$$H_{\rm eff} = \alpha_{\rm R}\boldsymbol{\sigma}\times\boldsymbol{k}\cdot I_z + \alpha_{\rm D}\boldsymbol{\sigma}\cdot\boldsymbol{k} + \left[\Delta - \frac{A^2}{\hbar\omega}(\alpha_{\rm R}^2 + \alpha_{\rm D}^2)\right]\sigma_z. \tag{9}$$

The last term in the above equation denotes that a photo-induced modulation of the gap would be possible.

In the clean limit, the intrinsic Hall conductivity can be obtained from[30–32]

$$\sigma_{xy} = \frac{e^2}{\hbar}\int \frac{{\rm d}^2\boldsymbol{k}}{(2\pi)^2}\Omega^z(\boldsymbol{k}), \tag{10}$$

where Ω_n is the momentum-space Berry curvature for the n-th band

$$\Omega_n(\boldsymbol{k}) = -\sum_{n'\neq n}\frac{2{\rm Im}\langle u_{n\boldsymbol{k}}|\hat{v}_x|u_{n'\boldsymbol{k}}\rangle\langle u_{n'\boldsymbol{k}}|\hat{v}_y|u_{n\boldsymbol{k}}\rangle}{(E_{n'}-E_n)^2}. \tag{11}$$

The summation is over all occupied bands below the bulk gap, and $\hat{v}_{x\,(y)}$ is the velocity operator along x (y) direction. The band dispersions relationship of the effective Hamiltonian and the the corresponding wave functions are obtained from Eqs. (2)–(4) by replacing Δ with

$$\Delta' = \Delta - \frac{A^2}{\hbar\omega}(\alpha_{\rm R}^2 + \alpha_{\rm D}^2).$$

When the chemical potential $E_{\rm f}$ is in positive energy or negative energy, we find

$$\sigma_{xy} = -\frac{e^2}{4\pi\hbar}\frac{\Delta - (A^2/\hbar\omega)\alpha_{\rm R}^2(\kappa^2+1)}{|E_{\rm f}|}\frac{\kappa^2-1}{|\kappa^2-1|}. \tag{12}$$

When the chemical potential is in the gap, we find

$$\sigma_{xy} = -\frac{e^2}{4\pi\hbar}\frac{\Delta - (A^2/\hbar\omega)\alpha_{\rm R}^2(\kappa^2+1)}{|\Delta - (A^2/\hbar\omega)\alpha_{\rm R}^2(\kappa^2+1)|}\frac{\kappa^2-1}{|\kappa^2-1|}. \tag{13}$$

The direct correspondence between the Chern number and the Hall conductance for two-dimensional (2D) insulators is characterized by: $\sigma_{xy} = Ce^2/h$. In Fig. 2(a), we show the band Chern numbers as functions of different externally tunable parameters (κ and A). Figure 2(b) shows that Chern numbers are plotted as a function of A for $\kappa = 0.5$ (dashed blue line) and $\kappa = 2$ (solid red line). A is measured in units of $\sqrt{\hbar\omega\Delta}/\alpha_{\rm R}$. Based on Eq. (13), the amplitude of Chern numbers is independent of the frequency. However, the sign of Chern numbers is dependent on the frequency, and the frequency follows the condition of high-frequency limit $\omega \gg \alpha$. κ and A allow us to tune the Chern number of the lower spin-degenerate bands of the effective Floquet Hamiltonian (9) between $C = 1/2$ and $C = -1/2$. The direction of Hall current can be controlled by illuminating with light and choosing the Rashba and Dresselhaus parameters due to the fact that they lead the change of sign of the Berry curvature of occupied states. The Berry curvature of occupied states is

$$\Omega(k) = \frac{\Delta'(1-\kappa^2)}{2\pi\alpha_{\rm R}} \times \int_0^{2\pi}{\rm d}\varphi\left[\frac{1}{k^2(\kappa^2+2\kappa\sin 2\varphi+1)^2 + (\Delta'/\alpha_{\rm R})^2}\right]^{3/2}. \tag{14}$$

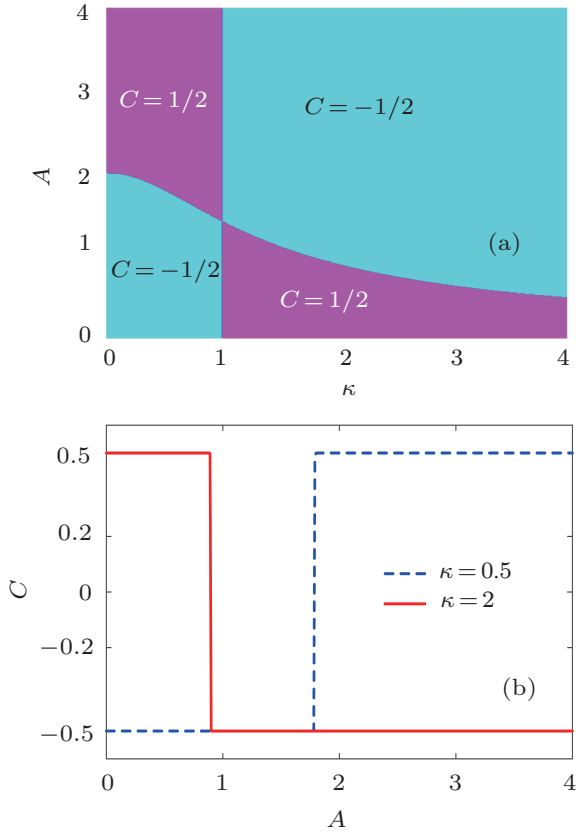


Fig. 2. (color online) (a) Phase diagram of periodically driven SmB_6 at a high-frequency regime for circularly polarized light in the (A, κ) plane. (b) Chern number as a function of A for $\kappa = 0.5$ and $\kappa = 2$. A is measured in units of $\sqrt{\hbar\omega\Delta}/\alpha_{\rm R}$, and $\omega \gg \alpha$.

The circularly polarized light breaks the time reversal symmetry and induces a gap term (see Eq. (9)). The band gap $(\Delta - (A^2/\hbar\omega)(\alpha_{\rm R}^2 + \alpha_{\rm D}^2))$ is closed and reopened along the change of Chern number between $C = 1/2$ and $C = -1/2$ for fixed κ when varying A, and the direction of the Hall current changed. For fixed A and varied κ, the varied κ changed the sign of Berry curvature, therefore the direction of Hall current changed with unchanged gap.

4. Transport properties in low-frequency regime

In the low-frequency regime, Flouqet theory cannot capture the effect of redistribution of electrons in the band structure. Within the relaxation time approximation, the Boltzmann transport equation for the electronic distribution function reads

$$\frac{\partial f_n(\boldsymbol{k},t)}{\partial t} - \frac{e}{\hbar}\boldsymbol{E}(t)\cdot\nabla_{\boldsymbol{k}} f_n(\boldsymbol{k},t) = -\frac{f_n(\boldsymbol{k},t) - f_0(E_n)}{\tau}, \quad (15)$$

where $f_0(E_n)$ is the Fermi–Dirac distribution for the n-th band energy of the system, $\boldsymbol{E}(t) = -\partial \boldsymbol{A}(t)/\partial t = E_0(\sin\omega t, -\cos\omega t)$, and τ is the relaxation time. We consider that the system is subjected to a weak finite ac field. Then the distribution to the linearized term has the form

$$f_n(\boldsymbol{k},t) = f_0(E_n) + g_n(\boldsymbol{k},t), \quad (16)$$

where $g_n(\boldsymbol{k},t)$ follows the differential equation

$$\frac{\partial g_n(\boldsymbol{k},t)}{\partial t} + \frac{g_n(\boldsymbol{k},t)}{\tau} = \frac{e}{\hbar}\boldsymbol{E}(t)\cdot\nabla_{\boldsymbol{k}} f_0(E_n). \quad (17)$$

After straightforward calculation, we obtain

$$g_n(\boldsymbol{k},t) = eE_0\frac{\partial f_0(E_n)}{\partial \varepsilon} \times \left[\frac{\partial E_n/\partial k_x - \mathrm{i}\partial E_n/\partial k_y}{2\mathrm{i}}\frac{\mathrm{e}^{\mathrm{i}\omega t}}{1/\tau + \mathrm{i}\omega} + \mathrm{H.c.}\right], \quad (18)$$

where $E_\pm = \pm\sqrt{\alpha^2 k^2 + \Delta'^2}|_{A=0}$.

The light-induced current in the system is expressed through

$$j_x = -\frac{e}{\hbar}\sum_n \int \frac{\mathrm{d}^2\boldsymbol{k}}{(2\pi)^2}\frac{\partial E_n}{\partial k_x} f_n(\boldsymbol{k},t). \quad (19)$$

Substituting Eq. (16) into Eq. (19) and performing integration, we obtain

$$j_x = \frac{e^2 E_0}{8\mathrm{i}\hbar\pi^2}\frac{\mathrm{e}^{\mathrm{i}\omega t}}{1/\tau + \mathrm{i}\omega}\frac{E_f^2 - \Delta^2}{E_\mathrm{f}}[1 + \Theta(E_\mathrm{f} - \Delta)]\,G(\kappa) + \mathrm{H.c.}, \quad (20)$$

where $\Theta(x)$ is the Heaviside function, and

$$G(\kappa) = \int \mathrm{d}\varphi \frac{(\kappa^2+1)\cos\varphi + 2\kappa\sin\varphi}{(\kappa^2 + 2\kappa\sin 2\varphi + 1)^2} \times \left[(\kappa^2+1)(\cos\varphi - i\sin\varphi) + 2\kappa(\sin\varphi - \mathrm{i}\cos\varphi)\right]. \quad (21)$$

The current can be divided into the linear and nonlinear on E_f. The linear term is nothing but Drude's-like result. The nonlinear term originates from the band gap Δ. The current is dependent on the parameter of κ. In Fig. 3, we show the current for fixed E_f in units of $e^2E_0/8\hbar\pi^2$ for $\kappa = 0, 0.5, 2$. The amplitude of current with $\kappa \neq 0$ is greatly enhanced compared to the current with $\kappa = 0$. The locations of nodal point and antinodal point are shifted. The current is determined by the group velocity

$$\frac{\partial E_\pm}{\partial k_{x,y}} = \pm\alpha_\mathrm{R} = \frac{(\kappa^2+1)k_{x,y} + 2\kappa k_{y,x}}{\sqrt{(\kappa^2 + 2\kappa\sin 2\varphi + 1)k^2 + \Delta^2}}. \quad (22)$$

We can find that the κ affected the group velocity, and the energy band dispersion (see Fig. 1) is also changed. Therefore, the light-induced current can be controlled by κ.

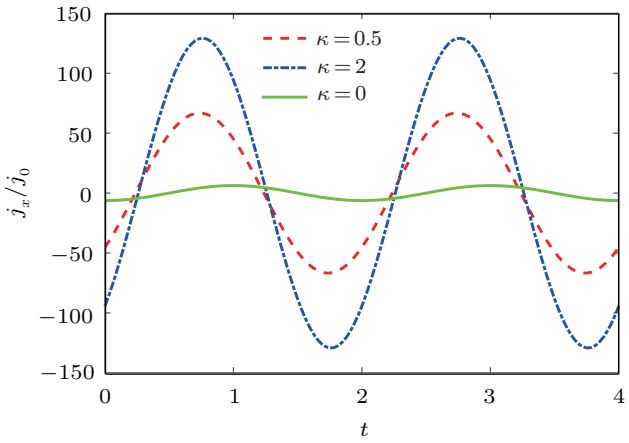


Fig. 3. (color online) Light-induced current plotted for $\kappa = 0, 0.5, 2$ in units of $j_0 = E_0(E_\mathrm{f}^2 - \Delta^2)/8E_\mathrm{f}\hbar\pi^2$.

5. Conclusion and summary

To conclude, we have analyzed transport properties of the $\overline{X}$ point in the Brillouin zone of the topological Kondo insulator SmB_6 under the application of a circularly polarized light. We have employed Floquet theory and Boltzmann equation to compute the Hall conductivity at high-frequency regime and the current at low-frequency regime as a function of the ratio (κ) of the Dresselhaus-like and Rashba-like spin–orbit parameters respectively. At high-frequency regime, Berry curvature can be reversed by the ratio κ and the amplitude of the light. Therefore, the direction of Hall current can be controlled by the choice of the Rashba and Dresselhaus parameters and the amplitude of the light. At low-frequency regime, the group velocity can be modified by the ratio κ. The amplitude of the light-induced current is enhanced due to the ratio κ. The locations of nodal point and antinodal point are also shifted. Our findings provide a way to control the transport properties of the Dirac materials. It is also important for studying the effect of spin–orbit coupling in the materials.

References

[1] Hasan M Z and Kane C L 2010 *Rev. Mod. Phys.* **83** 3045
[2] Qi X L and Zhang S C 2011 *Rev. Mod. Phys.* **83** 1057
[3] Takimoto T 2011 *J. Phys. Soc. Jpn.* **80** 123710
[4] Alexandrov V, Dzero M and Coleman P 2013 *Phys. Rev. Lett.* **111** 226403
[5] Lu F, Zhao J Z, Weng H, Fang Z and Dai X 2013 *Phys. Rev. Lett.* **110** 096401
[6] Dzero M, Sun K, Galitski V and Coleman P 2010 *Phys. Rev. Lett.* **104** 106408
[7] Kim D J, Xia J and Fisk Z 2014 *Nat. Mater.* **13** 466
[8] Yu R, Weng H, Hu X, Fang Z and Dai X 2015 *New J. Phys.* **17** 023012
[9] Erten O, Ghaemi P and Coleman P 2016 *Phys. Rev. Lett.* **116** 046403
[10] Zhang L, Song X Y and Wang F 2016 *Phys. Rev. Lett.* **116** 046404
[11] Kim J, Kim K, Kang C J, Choi H C, Kang J S, Denlinger J D and Min B I 2014 *Phys. Rev. B* **90** 075131

[12] Baruselli P P and Vojta M 2015 *Phys. Rev. Lett.* **115** 156404
[13] Legner M, Rüegg A and Sigrist M 2015 *Phys. Rev. Lett.* **115** 156405
[14] Wolgast S, Kurdak C, Sun K, Allen J W, Kim D J and Fisk Z 2013 *Phys. Rev. B* **88** 180405
[15] Kim D J, Thomas S, Grant T, Botimer J, Fisk Z and Xia J 2013 *Sci. Rep.* **3** 3150
[16] Zhang X, Butch N P, Syers P, Ziemak S, Greene R L and Paglione J 2013 *Phys. Rev. X* **3** 011011
[17] Syers P, Kim D, Fuhrer M S and Paglione J 2015 *Phys. Rev. Lett.* **114** 096601
[18] Xu N, Biswas P K, Dil J H, Dhaka R S, Landolt G, Muff S, Matt C E, Shi X, Plumb N C, Radović M, Pomjakushina E, Conder K, Amato A, Borisenko S V, Yu R, Weng H M, Fang Z, Dai X, Mesot J, Ding H and Shi M 2014 *Nat. Commun.* **5** 4566
[19] Kitagawa T, Oka T, Brataas A, Fu L and Demler E 2011 *Phys. Rev. B* **84** 235108
[20] Sengupta P, Matsubara M and Bellotti E 2015 arXiv **1509.08984** [cond-mat]
[21] Sengupta P and Bellotti E 2016 *App. Phys. Lett.* **108** 031101
[22] Lu H Z, Shi J R and Shen S Q 2011 *Phys. Rev. Lett.* **107** 076801
[23] Peres N M R 2010 *Rev. Mod. Phys.* **82** 2673
[24] Oka T and Aoki H 2009 *Phys. Rev. B* **79** 081406
[25] Lindner N H, Rafael G and Galitski V 2011 *Nat. Phys.* **7** 490
[26] Shirley J H 1965 *Phys. Rev.* **138** B979
[27] Sambe H 1973 *Phys. Rev. A* **7** 2203
[28] Grifoni M and Hänggi P 1998 *Phys. Rep.* **304** 229
[29] Kohler S, Lehmann J and Hänggi P 2005 *Phys. Rep.* **406** 379
[30] Yao Y, Kleinman L, MacDonald A H, Sinova J, Jungwirth T, Wang D, Wang E and Niu Q 2004 *Phys. Rev. Lett.* **92** 037204
[31] Zhang X M and Duan Y S 2010 *Chin. Rev. Lett.* **27** 077301
[32] Sun L and Wan S L 2015 *Chin. Rev. Lett.* **32** 057501